Molecular Therapy
Nucleic Acids
Original Article

LINC01094 promotes pancreatic cancer progression by sponging miR-577 to regulate LIN28B expression and the PI3K/AKT pathway

Chen Luo,[1,2,3] Kang Lin,[1,2,3] Cegui Hu,[1,2,3] Xiaojian Zhu,[1,2] Jinfeng Zhu,[1,2] and Zhengming Zhu[1]

[1]Department of General Surgery, Second Affiliated Hospital of Nanchang University, Nanchang, China; [2]Jiangxi Province Medical College of Nanchang University, Nanchang, China

The leading cause of death in pancreatic cancer (PC) patients is the progression of cancer metastasis. Recently, long non-coding RNAs (lncRNAs) have been shown to play an important role in regulating cancer cell proliferation and metastasis; however, its molecular basis in PC remains to be explored. In this study, we observed that LINC01094 was markedly overexpressed in PC tissues and was associated with poor patient prognosis. Downregulation of LINC01094 decreased the proliferation and metastasis of PC cells and inhibited tumorigenesis and metastasis in mouse xenografts. Mechanically, LINC01094 acted as an endogenous miR-577 sponge to increase the expression of its target gene, the RNA-binding protein lin-28 homolog B (LIN28B), by decoying the miR-577, thereby activating the PI3K/AKT pathway. Our findings suggest that LINC01094 plays critical roles in proliferation and metastasis of PC, implying that LINC01094 can be regarded as a new biomarker or therapeutic target for the treatment of PC.

INTRODUCTION

Pancreatic cancer (PC) is one of the most frequently diagnosed cancers and the fourth leading cause of cancer-related deaths in the United States.[1] Although the diagnosis and treatment of PC have made remarkable progress, the majority of PC patients have relapsed because of local infiltration or extensive metastasis.[2–5] Therefore, understanding the molecular regulation mechanism involved in the proliferation and metastasis of PC cells is urgently needed in the treatment of PC.

Long non-coding RNAs (lncRNAs) are a kind of RNA with a length longer than 200 nucleotides and that has no function in protein coding.[6–9] In recent years, lncRNAs have been found to play crucial roles in the recurrence, metastasis, and chemotherapy resistance of tumors.[10–13] For example, oncogenes Ras and Myc can promote tumorigenesis through lncRNA Orilnc1 and differentiation antagonizing noncoding RNA (DANCR), respectively.[14,15] Several kinds of lncRNA have been involved in the metastasis of cancers. In PC, the expression of lncRNAs are often maladjusted; for example, lncRNA highly upregulated in liver cancer (HULC) is abnormally increased in PC, and its high expression is significantly related to the metastasis and vascular invasion of PC.[16] In addition, lncRNA plasmacytoma variant translocation1 (PVT1) upregulates the progression and glycolysis of PC cells by regulating microRNA-519d-3p (miR-519d-3p) and Hypoxia-inducible factor 1 α (HIF1α), and LINC00657 acts as a miR-433 sponge to enhance the malignancy of pancreatic ductal adenocarcinoma.[17,18] Although lncRNA plays a decisive role in PC, the study of LINC01094 in PC has not been reported, and the interaction between LINC01094 and microRNA (miRNA) remains unclear. Previous studies have shown that LINC01094, as an miR-224-5p competing endogenous RNA (ceRNA), is an important anti-cancer miRNA that enhances the pathogenesis of renal cell carcinoma.[19] miRNAs have been considered crucial modulators in tumors, and Zhang et al.[20] found miR-577 to be correlated with the formation and progression in glioblastoma and liver cancers.[21]

The RNA-binding protein lin-28 homolog B (Lin28B) is a homolog of Lin28,[22] which was first identified in the nematode *Caenorhabditis elegans*, and has an essential function in advanced human malignancies including PC.[23,24] It is found that Lin28B could selectively block the expression of let-7 miRNAs.[25] The upregulation of Lin28B decreased let-7 levels and activated the phosphatidylinositol 3-kinase/protein kinase B (PI3K/AKT) pathway in PC then activated the transcription of target genes including Myc, proliferating cell nuclear antigen (PCNA), and matrix metalloproteinase 9 (MMP9).[26,27] The role of the PI3K/AKT pathway in malignant diseases has been widely studied, and altered expression or mutation of many components of this pathway has been implicated in human cancer.[28,29] However, it remains unclear whether and how lncRNAs are involved in the metastasis of PC by regulating the PI3K/AKT pathway. Therefore, in this study, we investigated the clinical significance of LINC01094 expression in PC and obtained insights into the function and mechanisms underlying LINC01094 regulation of PC proliferation and metastasis.

Received 24 January 2021; accepted 20 August 2021;
https://doi.org/10.1016/j.omtn.2021.08.024.

[3]These authors contributed equally

Correspondence: Zhengming Zhu, Department of General Surgery, Second Affiliation Hospital of Nanching University, Nanchang, China.
E-mail: zzm8654@163.com

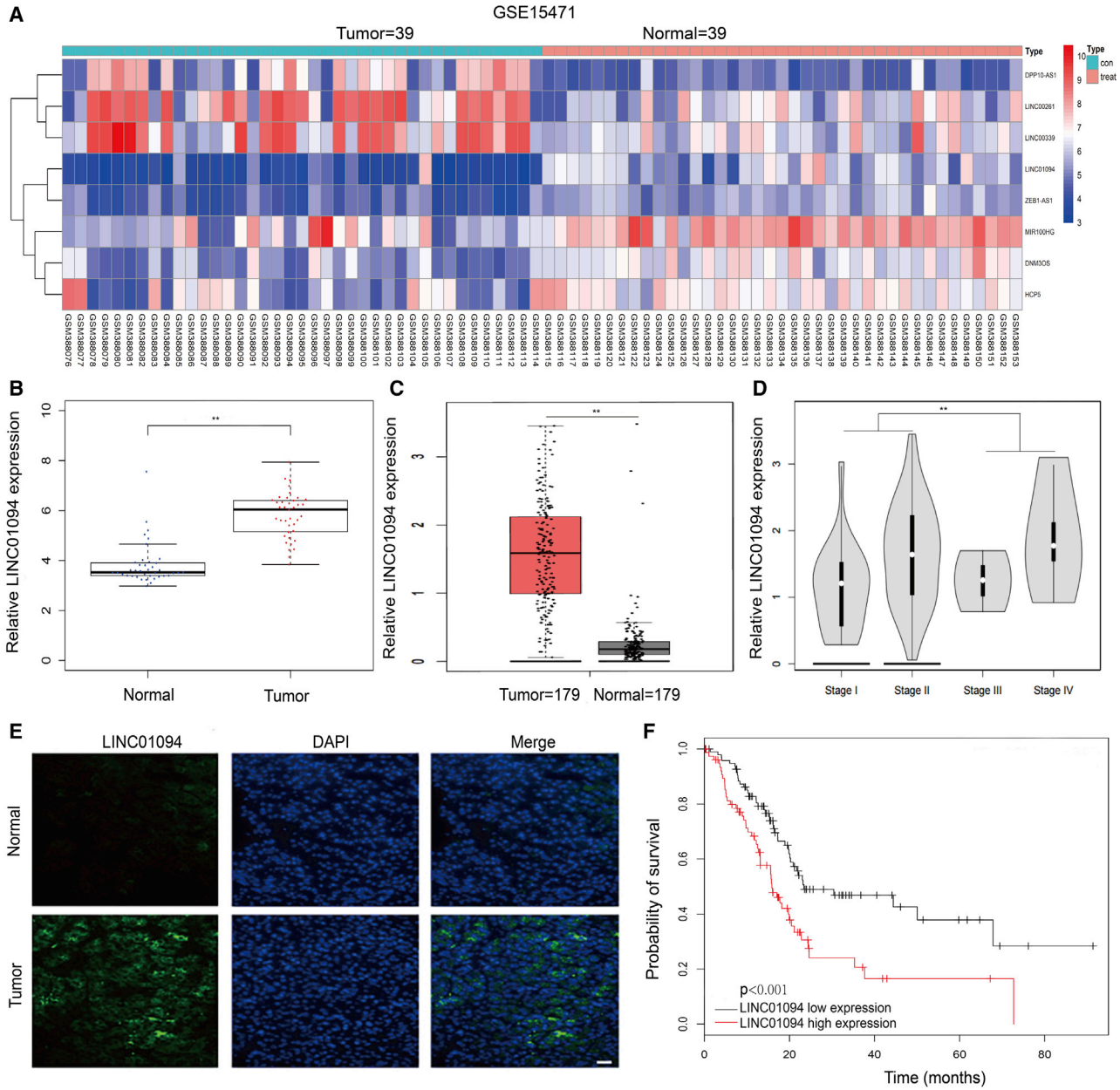

Figure 1. LINC01094 is upregulated in PC and is associated with poor prognosis

(A) Heatmaps of lncRNAs that were differentially expressed between pancreatic cancer (PC) tissues and matched adjacent normal samples. The color scale shown illustrates the relative RNA expression levels; red represents high expression and blue represents low expression. (B) Relative expression of LINC01094 in GEO: GSE15471 dataset. (C) The mRNA expression of LINC01094 in PC and normal pancreatic tissues from the TCGA database (**p < 0.01). (D) Relative LINC01094 expression in PC tissues with different TNM stage (p = 0.0191). (E) FISH was used to determine the expression of LINC01094 in PC tissue and the paired non-tumor sample (scale bar, 100 μm). (F) Kaplan-Meier analysis of survival time with LINC01094 high and low levels in PC patients from TCGA database (p = 0.00071, log-rank test).

RESULTS

LINC01094 is upregulated in PC and is associated with poor prognosis

To identify the abnormally expressed lncRNAs in PC, we used the basic local alignment search tool (BLAST) program, through U133PLUS2.0 technology, to analyze Gene Expression Omnibus (GEO): GSE15471, which is comprised of lncRNA data for 39 PC tissues and 39 neighboring non-tumor control tissues. Of note, PC tissues expressed 8 notably differentially expressed lncRNAs as compared with neighboring non-tumor tissues (Figure 1A). Among them,

Table 1. The correlation between the clinicopathological characteristics and LINC01094 expression in 91 PC patients

Characteristics	No. of patients	LINC01094 expression		**p
		Low n = 33	High n = 58	
Age (year)				
<60	49	19	30	0.59
≥60	42	14	28	
Gender				
Female	37	15	22	0.482
Male	54	18	36	
Tumor size (mm)				
<30	57	15	42	0.011*
≥30	34	18	16	
Location				
Head/neck	45	17	28	0.776
Body/tail	46	16	30	
Lymphatic metastasis				
Positive	53	12	41	0.001**
Negative	38	21	17	
Distant metastasis				
Positive	41	9	32	0.01*
Negative	50	24	26	
TNM stage				
I/II	41	20	21	0.025*
III/IV	50	13	37	

*p < 0.05, ** p < 0.01.

LINC01094 was one of the most significantly upregulated lncRNAs in the datasets. In addition, quantitative real-time PCR analysis showed that LINC01094 expression was higher in PC tissues than in non-tumor tissues from GEO: GSE15471 and The Cancer Genome Atlas (TCGA) database (Figures 1B and 1C, **p < 0.01). Moreover, the level of LINC01094 in advanced PC (stages III and IV) was upregulated compared with early-stage PC (stages I and II) (Figure 1D, **p < 0.01). A fluorescence *in situ* hybridization (FISH) assay verified the overexpression of LINC00194 in PC tissues compared to the non-tumor samples (Figure 1E). Next, we evaluated the relationship between LINC01094 levels and clinicopathological features of PC (Table 1). This analysis indicated that the high level of LINC01094 correlated with tumor size (*p < 0.05), lymph node metastasis (**p < 0.01), and tumor-node-metastasis (TNM) stages (*p < 0.05). Kaplan-Meier survival analysis revealed that a high level of LINC01094 was associated with the poor survival rate of patients with PC from TCGA database (Figure 1F, p = 0.00071). In addition, univariate analysis indicated that tumor size, lymphatic metastasis, TNM classification, and LINC01094 expression were noteworthy predictors of overall survival in PC patients (Table 2, **p < 0.01). Multivariate analysis showed that LINC01094 was an independent protective predictor of overall survival (Table 2, **p < 0.01). In addition, tumor size, lymphatic metastasis, TNM classification also were independent risk predictors of overall survival in PC patients (Table 2, *p < 0.05, **p < 0.01). Taken together, these results indicated that high LINC01094 expression is associated with poor prognosis, highlighting the potential for LINC01094 as an independent prognostic marker in PC.

LINC01094 promotes the proliferation of PC cells *in vitro*

Next, we analyzed LINC01094 expression in a normal pancreatic cell (HPDE6-C7) and PC cell (CFPAC-1, BXPC-3, ASPC-1, PANC-1, and SW1990) lines. The results showed that LINC01094 expression in BXPC-3, ASPC-1, and PANC-1 cells was higher than in normal cells (Figure 2A, *p < 0.05, **p < 0.01, not significant [ns] p > 0.05). Then, ASPC-1 and PANC-1 cells with the high level of LINC01094 were selected to transfect siRNA-LINC01094#1 (siLINC01094#1 group), siRNA-LINC01094#2 (siLINC01094#2 group), and negative control sequence (siNC) (Figure 2B). Downregulation of LINC01094 decreased the colony formation capacity and cell growth of PC (Figures 2C and 2D, **p < 0.01). In contrast, overexpression of LINC01094 significantly enhanced the proliferation of CFPAC-1 cells (Figures S2B and S2C, **p < 0.01). Western blot analysis showed that silencing of LINC01094 in PANC-1 and ASPC-1 cells inhibited PCNA expression, a factor known to promote cell proliferation (Figure 2E), while overexpression of LINC01094 did the opposite (Figure S2F, **p < 0.01). Taken together, these datasets suggest that LINC01094 may promote PC progression.

LINC01094 promotes PC cell metastasis *in vitro*

To explore the function of LINC01094 in PC cell metastasis, we designed wound-healing and transwell experiments in PANC-1 and ASPC-1 cells. The results showed that downregulation of LINC01094 decreased the migration and invasion ability of PC cells and suggested that growth and survival of PANC-1 cells were affected more than that of ASPC-1 cells (Figures 3A and B, **p < 0.01). However, overexpression of LINC01094 significantly increased the migration and invasion ability of CFPAC-1 cells (Figures S2D and S2E, **p < 0.01). Western blot analysis showed that silencing of LINC01094 in PANC-1 and ASPC-1 cells inhibited MMP9 expression, which promotes cell metastasis (Figure 3C), while overexpression of LINC01094 enhanced MMP9 (Figure S2F, **p < 0.01). Taken together, these data suggest that LINC01094 may promote PC progression.

LINC01094 acts as miRNA sponge for miR-577

lncRNAs could recruit miRNAs to function as ceRNAs during oncogenesis.[30] To verify whether LINC01094 had a similar function in PC cells, lncRNA subcellular localization predictor (lncLocator, http://www.csbio.sjtu.edu.cn/bioinf/lncLocator/) was used to predict its localization in cells, and subcellular fractionation was performed for confirmation. Data showed that LINC01094 was mainly localized to the cytoplasm (Figures 4A, 4B, and S4A). In addition, FISH results suggested that LINC01094 mainly located in the cytoplasm (Figures 4C and S4B), indicating that LINC01094 might regulate target protein expression at the posttranscriptional level. Next, we used the bioinformatics databases starBase (http://starbase.sysu.edu.cn/) to predict the potential miRNAs (Table S2). According to the predicted result, there

Table 2. Univariate and multivariate analyses of survival in 91 PC patients (Cox proportional hazards regression model)

Variables		Univariate analysis			Multivariate analysis		
		HR	95% CI	p value	HR	95% CI	p value
Age (≥60 versus <60)		1.304	0.763–2.228	0.331	–	–	–
Gender (male versus female)		1.127	0.646–1.966	0.673	–	–	–
Tumor size (cm) (≥3 versus <3)		2.622	1.516–4.535	0.001**	2.108	1.147–3.874	0.016*
Location							
	head/neck versus Body/tail	1.459	0.854–2.492	0.167	–	–	–
	Lymphatic metastasis (positive versus negative)	7.992	3.809–16.77	<0.001**	6.313	2.60–15.327	0.001**
	Distant metastasis (positive versus negative)	6.346	2.718–14.816	<0.001**	2.496	1.336–4.664	0.004**
	TNM staging (I/II versus III/IV)	6.58	3.604–12.013	<0.001**	3.039	1.501–6.151	0.002**
	LINC01094 expression (high versus low)	5.181	2.544–10.552	<0.001**	3.644	1.439–9.223	0.006**

*p < 0.05, ** p < 0.01.

were three miRNAs (miR-577, miR-330-3p, and miR-545-3p) for whom LINC01094 contained multiple binding sites. Quantitative real-time PCR analysis was used to detect the expression of the three miRNAs in PC cells downregulated by shLINC01094 and upregulated by LINC01094, and only miR-577 changed (Figures 4D and S4C, **p < 0.01). In addition, LINC01094 expression did not change after knockdown of miR-577 (Figures 4E and S4D, ns, p > 0.05). Therefore, we regarded miR-577 as the main candidate for further research. To verify the direct binding of LINC01094 and miR-577 at the endogenous level, a luciferase reporter analysis was conducted, which included LINC01094 binding sites of wild-type (WT) or mutant (Mut) (Figure 4F, **p < 0.01). The results indicated that miR-577/mimic increased the luciferase activity of a WT-LINC01094 reporter vector; however, the luciferase activity of Mut-LINC01094 reporter vector did not increase (Figures 4G and S4E, **p < 0.01). It was well known that miRNAs bound to its target and caused translation inhibition and RNA degradation in an Ago2 dependent manner.[31] To further validate the potential binding of LINC01094 to miR-577, an RNA immunoprecipitation (RIP) assay using an anti-Ago2 antibody was performed. The data exhibited that both LINC01094 and miR-577 were obviously enriched in Ago2 complex (Figures 4H and S4F, **p < 0.01), which identified that LINC01094 might act as a ceRNA to regulate miR-577. In addition, we found that the expression of miR-577 in normal pancreatic cells and adjacent normal tissues were higher than that in PC cells and PC tissues (Figures 4I and J, *p < 0.05, **p < 0.01) and negatively correlated with LINC01094 (Figure 4K, r = −0.6024, **p < 0.01). Moreover, low miR-577 expression predicted a poor prognosis in PC patients (Figure 4L, p = 0.0017).

LIN28B is a downstream target of miR-577

To explore the downstream target of miR-577, we analyzed five miRNA datasets and then looked for the potential miR-577 target genes in all of them (Figure 5A). Also, we analyzed miR-577 expression in a normal pancreatic cell (HPDE6-C7) and PC cell lines (CFPAC-1, BXPC-3, ASPC-1, PANC-1, and SW1990). The results showed that miR-577 expression in PANC-1 cells was lower than in other cells and miR-577 expression in CFPAC-1 cells was higher (Figure 4I, **p < 0.01). So, PANC-1 and ASPC-1 cells with the low level of miR-577 were selected to transfect miR-577/inhibitor, and CFPAC-1 cells with the high level of miR-577 were selected to transfect miR-577/mimic, followed by quantitative real-time PCR analysis of the four targets, where we found that only LIN28B changed (Figures 5B and S5A). To verify the direct binding of LIN28B and miR-577 at the endogenous level, a luciferase reporter analysis was designed, which included LIN28B binding sites of WT or Mut syndrome. The results indicated that miR-577/mimic decreased the luciferase activity of the WT-LIN28B reporter vector; however, the luciferase activity of the Mut-LIN28B reporter vector did not decrease (Figures 5C, 5D, and S5B). To further illustrate the potential interaction between LIN28B and miR-577, miR-577 mimic was transfected into PANC-1 and ASPC-1 cells, followed with a quantitative real-time PCR and western blot analysis. The results showed that LIN28B mRNA and protein levels were significantly downregulated (Figures 5E, 5F, S5C, and S5D, **p < 0.01). Moreover, western blot analysis showed that the silencing of miR-577 in CFPAC-1 cells promoted MMP9, PCNA, and LIN28B expression, factors known to promote cell proliferation and metastasis, while overexpression of miR-577 inhibited their expression (Figure 5F, **p < 0.01). Plate-cloning and 5-Ethynyl-2′-deoxyuridine (EdU) assays showed that miR-577 overexpression could significantly decrease colony formation and growth. In contrast, silencing of miR-577 promoted colony formation and growth in CFPAC-1 cells (Figures 5G, 5H, S5E, and S5F, **p < 0.01). Wound-healing and transwell assays also showed that miR-577 overexpression could significantly decrease the ability of metastasis in PANC-1 cells, however, downregulation of miR-577 had the opposite effect in CFPAC-1 cells (Figures 5I, 5J, S5G, and S5H, **p < 0.01). Additionally, we found that the expression of LIN28B was highly expressed in PC tissues compared with non-tumor tissues (Figures 5K and 5L, **p < 0.01) and negatively correlated with LINC01094 (Figure 5M, r = 0.4918, **p < 0.01).

LINC01094 acts as a sponge of miR-577 to upregulate LIN28B expression

Since LINC01094 could inhibit miR-577 expression, we then determined whether LINC10094 could affect the expression of LIN28B

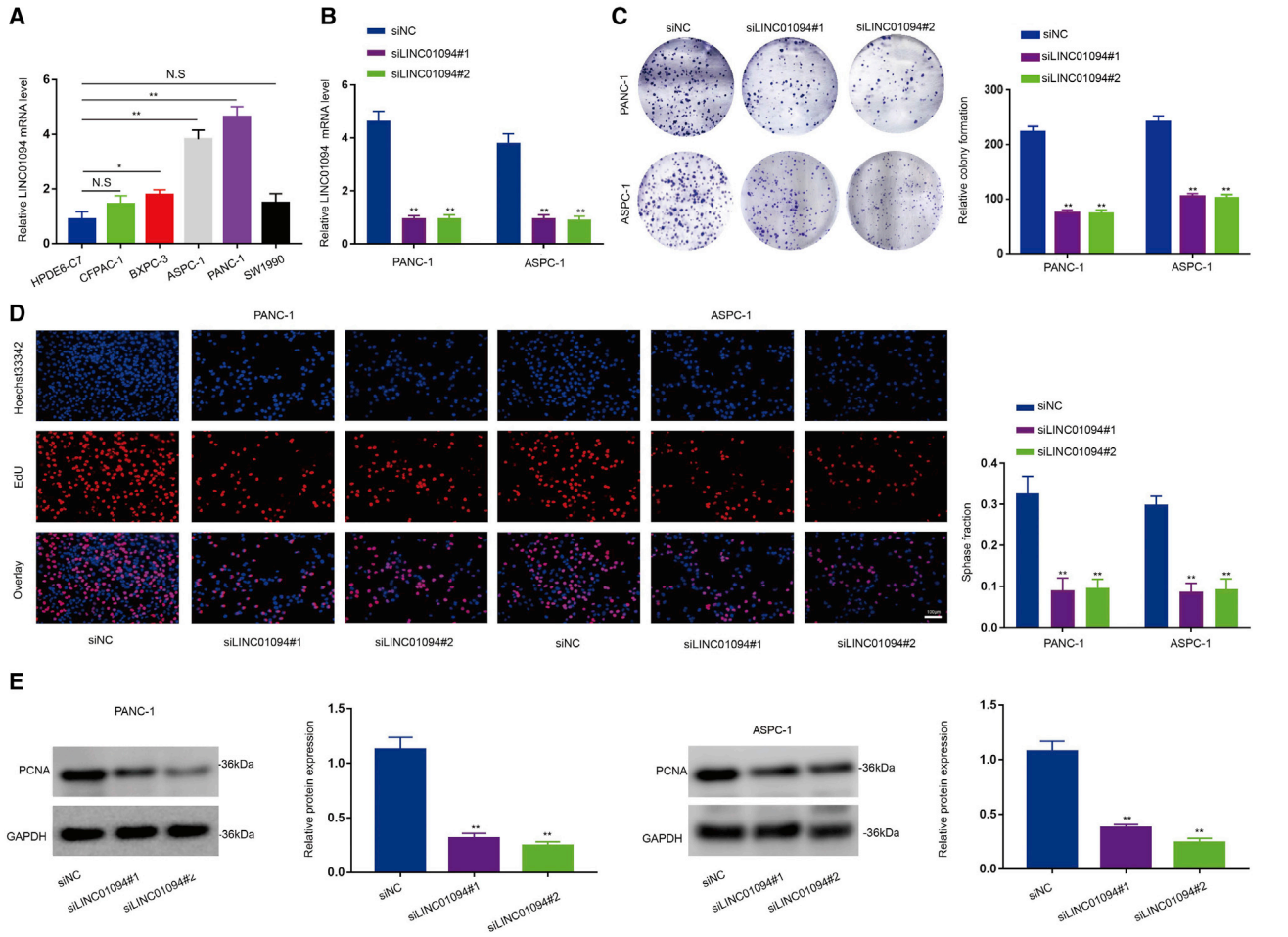

Figure 2. LINC01094 promotes the proliferation of PC cells *in vitro*

(A) LINC01094 mRNA expression was analyzed in PC cells and normal pancreatic cells. (B) LINC01094 mRNA expression was analyzed in PANC-1 and ASPC-1 cells stably transfected with siNC, siLINC01094#1, and siLINC01094#2 (**p < 0.01). (C and D) LINC01094 knockdown decreased cell viability and colony formation capacity in PANC-1 cells (**p < 0.01; scale bar, 100 μm). (E) Western blot to detect proliferation-associated antigen PCNA expression in PANC-1 and ASPC-1 cells stably transfected with siNC, siLINC01094#1, and siLINC01094#2 (**p < 0.01); data were expressed as mean ± SD and analyzed using unpaired t test. The experiment was repeated three times.

through competitive binding with miR-577. To this end, rescue experiments were designed using miR-577 inhibitors and mimics. As expected, western blot assays demonstrated that knockdown of LINC01094 decreased the protein levels of LIN28B, PCNA, and MMP9 in PANC-1 cells, while upregulation of LINC01094 enhanced the levels of LIN28B, PCNA, and MMP9 in CFPAC-1 cells (Figure 6A, **p < 0.01). Simultaneously, the effects caused by silencing or overexpressing LINC01094 were reversed by miR-577 inhibitors or mimics, respectively (Figures 6A and S6A, **p < 0.01). Moreover, plate-cloning and EdU assays showed that the miR-577 inhibitor reversed the proliferation-, migration-, and invasion-suppressing effects induced by knockdown of LINC01094 in PANC-1 and ASPC-1 cells, whereas miR-577 mimics counteracted the promoting effects induced by overexpression of LINC01094 in CFPAC-1 cells by colony formation, EdU, wound-healing, and transwell assays (Figures 6B–6E and S6B–S6E, **p < 0.01). To investigate whether LINC01094 exerts tumor-promoting functions in PC by modulating the miR-577/LIN28B axis, we then checked the effects of LIN28B on LINC01094-induced cell proliferation and metastasis by colony formation, EdU, wound-healing, and transwell assays (Figures S3B–S3E, **p < 0.01) and observed that LIN28B knockdown blocked the LINC00194-induced proliferation, migration, and invasion of PC cells. Next, western blotting was performed to investigate whether LIN28B affects MMP9 and PCNA levels in the context of LINC01094-driven cell proliferation and metastasis. The results showed that the extent of PCNA and MMP9 expression in the PANC-1 and ASPC-1 cells in the shLIN28B group was significantly lower than those levels in the shNCs (Figures S8A and S8B, **p < 0.01), but it significantly reversed the effects of LINC01094 overexpression on MMP9 and PCNA expression (Figure S3A, **p < 0.01). Collectively, these data demonstrated that LINC01094 served as a ceRNA for miR-577 to regulate LIN28B expression, thus leading to the progression and development of PC.

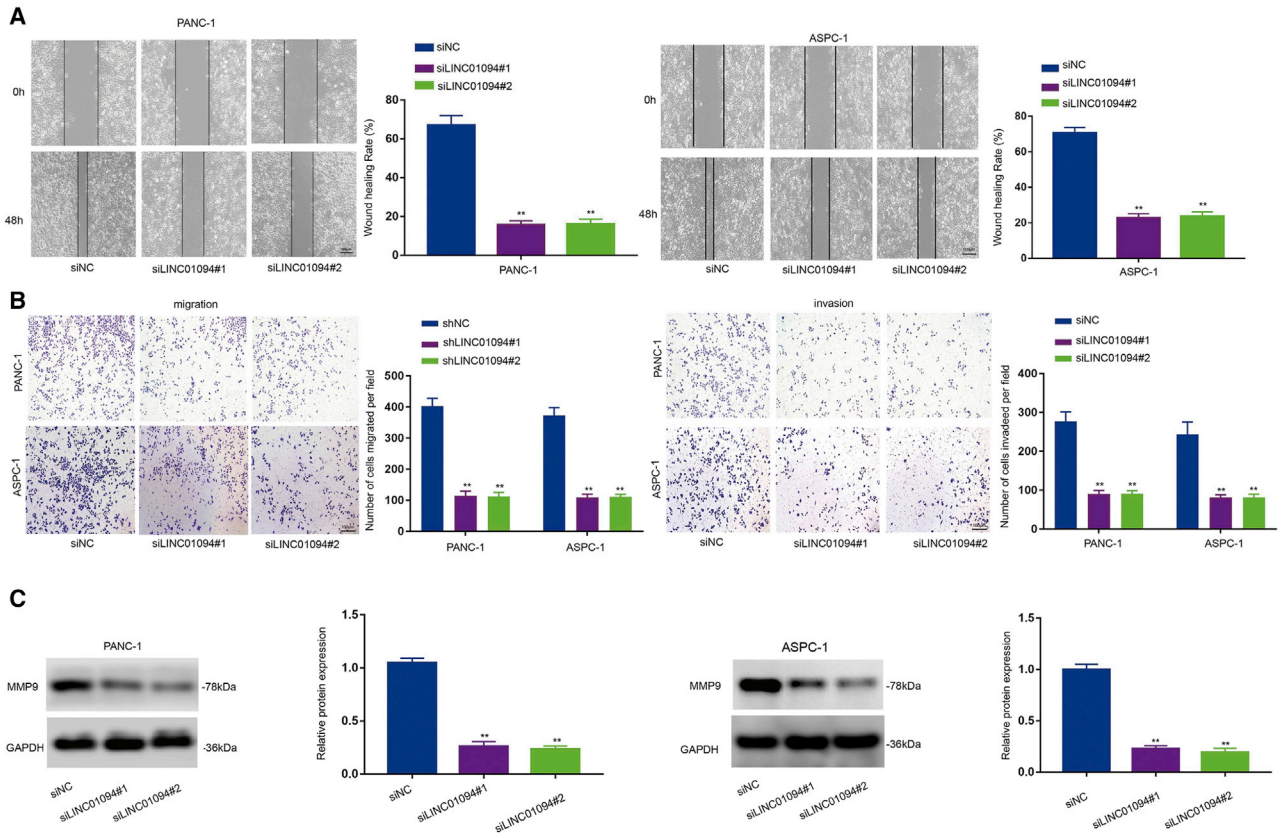

Figure 3. LINC01094 promotes PC cell metastasis *in vitro*

(A and B) Metastasis ability was measured using wound-healing (A) and transwell (B) assays in PC cells transfected with siNC, siLINC01094#1, and siLINC01094#2 (**p < 0.01; scale bar, 100 μm). (C) Western blot to detect proliferation-associated antigen MMP9 expression in PANC-1 and ASPC-1 cells stably transfected with siNC, siLINC01094#1, and siLINC01094#2 (**p < 0.01); data were expressed as mean ± SD and analyzed using unpaired t test. The experiment was repeated three times.

Silencing of LINC01094 suppresses the proliferation and metastasis of PC cells *in vivo*

In order to verify whether the LINC01094 affected the growth of PC *in vivo*, we constructed LINC01094-stable knockdown in PANC-1 cells using a lentivirus carrying short hairpin RNA (shRNA; shLINC01094) and LINC01094 stable overexpression in CFPAC-1 cells using a lentivirus carrying LINC01094 (LV-LINC01094) into BALB/c-free nude (male, 6–8 weeks). Compared with the shNC, the tumor growth and body weight of the shLINC01094 was significantly reduced (Figures 7A–7C and S7A–S7C, **p < 0.01). These subcutaneous tumor tissues were further utilized for western blot assays, and results of western blot and IHC assays showed the expression of LIN28B, PCNA, and MMP9 was downregulated in the shLINC01094 group compared to the shNC group, and the expression of LIN28B, PCNA, and MMP9 was upregulated in the LV-LINC01094 group compared to the vector group (Figures 7D, 7F, S7D, and S7F, **p < 0.01). Moreover, quantitative real-time PCR analysis of miR-577 were done in these subcutaneous tumor tissues. The result showed that the expression of miR-577 was upregulated in the shLINC01094 group compared to the shNC group, and the expression of miR-577 was downregulated in the LV-LINC01094 group compared to the vector group (Figures 7E and S7E, **p < 0.01). To investigate whether LINC01094 affected the invasion and migration of PC *in vivo*, we constructed LINC01094-stable knockdown in PANC-1 cells using a lentivirus carrying shRNA (shLINC01094) and LINC01094-stable high expression in CFPAC-1 cells using a lentivirus carrying LINC01094 (LV-LINC01094) into BALB/c-free male nude mice. Compared to the shNC, the metastatic nodules decreased in liver and lung, while, on the contrary, compared to the vector, the metastatic nodules increased in liver and lung (Figures 7F, 7G, S7F, and S7G, **p < 0.01). Furthermore, mice of the PANC-1-shLINC01094 group survived longer than controls, while, on the contrary, mice of the CFPAC-1-LV-LINC01094 group survived shorter than controls (Figures 7I, p = 0.00126, and S7F, p = 0.0378). These data demonstrated that LINC01094 can promote PC cell proliferation and metastasis in *vivo*.

Silencing LINC01094 suppresses the expression of the PI3K/Akt signaling pathway in PC cells

A previous study showed that the LIN28B can regulate the PI3K/Akt signaling pathway.[24] Moreover, the PI3K/Akt signaling pathway is involved in the regulation of tumor cell proliferation and metastasis, and PCNA and MMP-9 were the downstream target gene of the

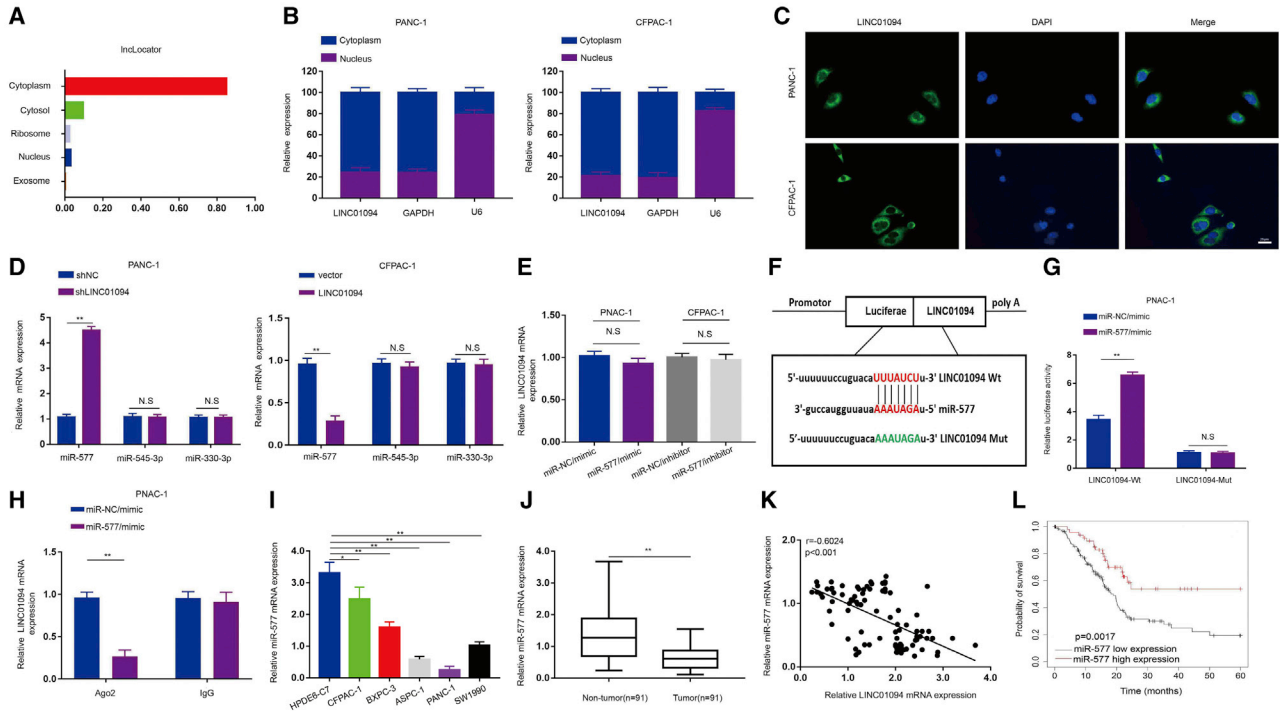

Figure 4. LINC01094 acts as miRNA sponge for miR-577

(A and B) LINC01094 localization was predicted using the lncRNA subcellular localization predictor lncLocator. (C) Fluorescence *in situ* hybridization (FISH) assay was conducted to determine the subcellular localization of LINC01094 in PANC-1 cells. Nuclei are stained blue (DAPI) and LINC01094 is stained green (scale bars, 25 μm). (D) Three miRNAs were predicted from starBase, and the expression levels of the three miRNAs were detected in cells transfected with LINC01094 expression vector or shLINC01094 (**p < 0.01; ns, not significant). (E) The expression of LINC01094 was analyzed in cells stably transfected with miR-577/mimic or miR-577/inhibitor (**p < 0.01; ns). (F) The putative miR-577 binding sites with the LINC01094 sequence 3′ untranslated region (3′ UTR) are shown. (G) Luciferase activity in PANC-1 cells co-transfected with miR-NC/mimic and miR-577/mimic containing LINC01094-WT and LINC01094-Mut. (H) RNA-IP with anti-antibodies was performed in PANC-1 cells transfected with miR-NC/mimic and miR-577/mimic (**p < 0.01; ns). (I) miR-577 mRNA expression was analyzed in the PC cells and a normal pancreatic cell. (J) The expression levels of miR-577 in 91 pairs of PC and in adjacent non-tumor tissues (**p < 0.01). (K) Scatterplots show a positive correlation between LINC01094 and miR-577 at the mRNA levels in 91 PC tissues (r = −0.6024, *p < 0.05, **p < 0.01). (L) Kaplan-Meier analysis of survival time with miR-577 high and low levels in PC patients from TCGA database (p = 0.0017); those among multiple groups were analyzed by the one-way ANOVA or repeated-measures ANOVA. Correlation analysis between two groups was conducted using Pearson's correlation analysis. The experiment was repeated three times.

PI3K/Akt signaling pathway.[25] To confirm the predicted results, a western blot was used to detect the PI3K/Akt protein level and phosphorylation. The results showed that the extent of LIN28B, PCNA, and MMP9 expression and PI3K/Akt phosphorylation in the PANC-1 and ASPC-1 cells in the shLINC01094 group was significantly lower than those levels in the shNC ($p < 0.05$), but the total protein levels of Akt and PI3K were not significantly changed in the shLINC01094 group (ns, $p > 0.05$, Figure 8C), while, on the contrary, the extent of LIN28B, PCNA, and MMP9 expression and PI3K/Akt phosphorylation in the CFPAC-1 cells in the LV-LINC01094 group was significantly higher than those levels in the vector ($p < 0.05$), but the total protein levels of Akt and PI3K were not significantly changed in the LV-LINC01094 group (ns, $p > 0.05$, Figure 8D). These data demonstrated that LINC01094 can activate PI3K/Akt signaling pathway in PC cells.

DISCUSSION

In recent years, more and more studies report that lncRNAs are associated with the progression of cancers.[32–34] For example, in PC, lncRNA pancreatic cancer associated transcript 1 (PLACT1) promoted growth and metastasis of pancreatic ductal carcinoma cells via the inhibitory κBα (IκBα)/E2F transcription factor 1 (E2F1) axis.[35] Another lncRNA, ENSGO0000254041.1, promoted pancreatic ductal carcinoma cells invasion, which was related to the poor prognosis of patients.[36] LINC01094 was first described in renal cell carcinoma and promoted the development of clear cell renal carcinoma through the miR-224-5p/chondroitin sulfate synthase 1 (CHSY1) axis.[19] However, the function of LINC01094 in PC had not been well studied. In this study, we screened the TGCA database, and bioinformatics analysis of GEPIA (Gene Expression Profiling Interactive Analysis) data showed that a new type of lncRNA, LINC01094, was found to have high expression in PC tissues but to be associated with poor prognosis and diminished survival time. In addition, knockdown of LINC01094 inhibited PC cell growth and metastasis ability.

Increasing evidence showed that there were extensive interaction networks involving ceRNA, in which lncRNA could regulate the

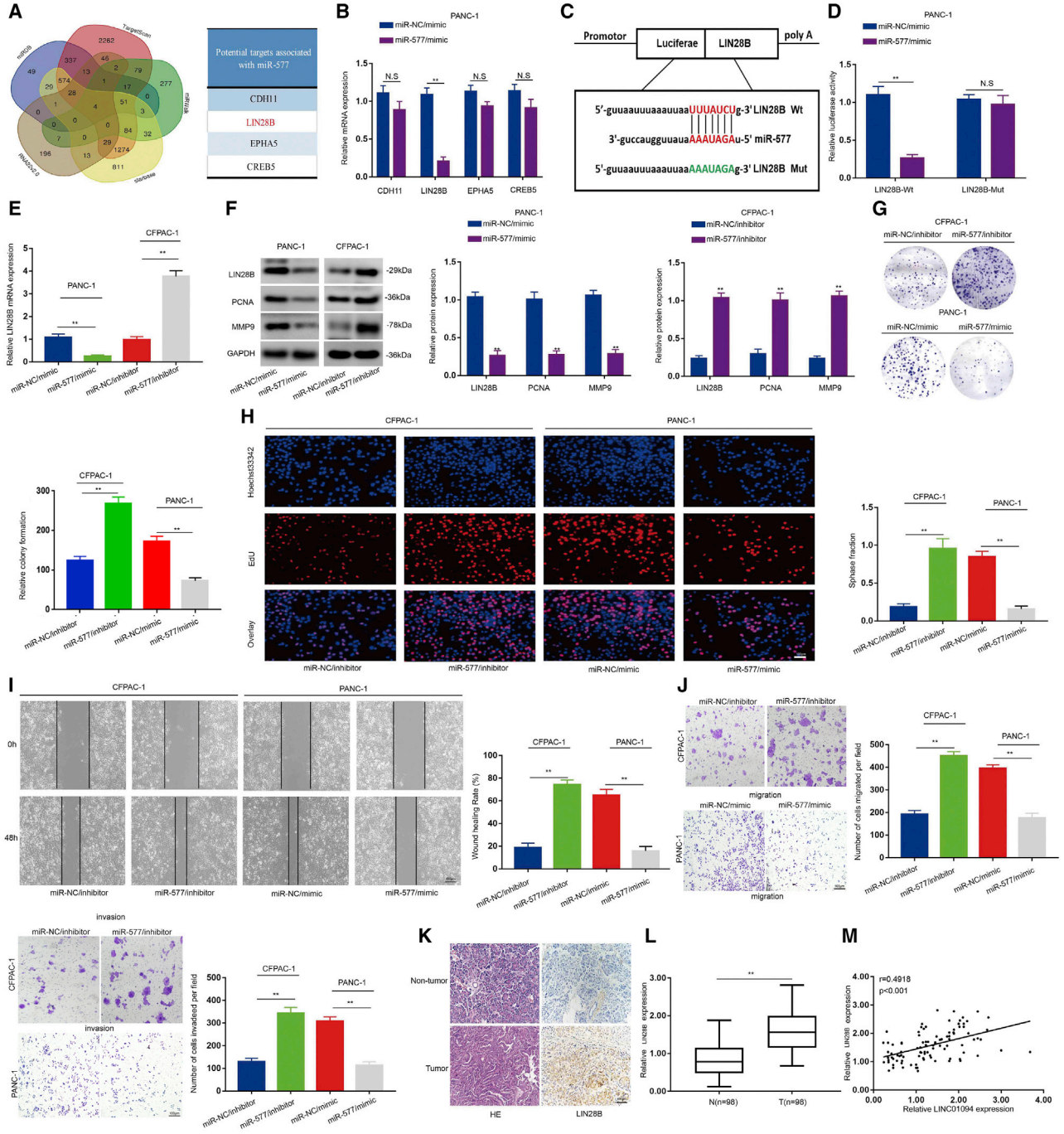

Figure 5. LIN28B is a downstream target of miR-577

(A) Potential targets of miR-577 predicted with five miRNA target databases. (B) Quantitative real-time PCR analysis for the 4 predicted targets of miR-577 in PANC-1 cells transfected with miR-577/mimics (**$p < 0.01$; ns). (C) The putative miR-577 binding sites with the LIN28B sequence 3′-UTR were shown. (D) Luciferase reporter gene activity of chimeric vectors carrying luciferase gene and LIN28B 3′-UTR fragments containing WT-LIN28B or Mut-LIN28B binding sites (**$p < 0.01$; ns). (E) LIN28B mRNA and protein expression were analyzed in PANC-1 and CFPAC-1 cells transfected with miR-577/mimic and miR-577/inhibitor (**$p < 0.01$). (F) Western blot to detect proliferation-associated antigen PCNA, MMP9, and LIN28B expression in PC cells stably transfected with miR-NC/mimic and miR-577/mimic and miR-NC/inhibitor and miR-577/inhibitor (**$p < 0.01$). (G and H) PC cell proliferation was measured using clone formation (G) and EdU (H) assays in PC cells transfected with miR-NC/mimic and miR-577/mimic

(legend continued on next page)

target RNA by binding to it and titrating from the binding site on the protein-coding messenger.[37,38] Target molecules regulated mutual expression by competing to bind miRNA's response element (MRE).[39] Evidence suggested that the ceRNA regulatory model had been validated in other cancers. For example, lncRNA miR-31 host gene (MIR31HG) inhibited the proliferation and metastasis of PC and caused sponge miR-575 to slightly regulate the expression of suppression of tumorigenicity 7 like (ST7L).[40] LINC00473 played a key role, because ceRNA regulated mitogen-activated protein kinase 1 (MAPK1) expression by turning miR-198 into a sponge.[41] Bioinformatics analysis, fluorescence reporter gene detection, and RIP analysis indicated that miR-577 was the target of LINC01094. Based on the previous research and functional analysis of LINC01094, we chose miR-577 for further research. The results showed that knocking down LINC01094 in PC cells could upregulate the expression of miR-577, and the LINC01094 expression did not change after knocking down miR-577. Then, we used bioinformatics analysis to predict miR-577 targets, and LIN28B was the most significantly downregulated target gene of miR-577. LIN28B, an RNA-binding protein, functions as an oncogene and is a potential therapeutic target for cancer.[42,43] Previous reports have proven that LIN28B is target of miR-30a-5p and that upregulation of LIN28B promotes tumor growth in breast cancers.[44] Moreover, miR-577 acts as a suppressor in many cancers, including glioblastoma and liver cancers.[20,21] In this study, our findings indicated that miR-577 inhibition increased PC growth and metastasis. Moreover, a recovery assay showed that LINC01094 affected PC cells growth and metastasis in a partially miR-577 dependent manner *in vitro*. Furthermore, the mechanism of the involvement of the PI3K/Akt signaling pathway in PC was investigated. We found that PANC-1 and ASPC-1 cells infected with LINC01094-shRNA presented decreased levels of p-Akt and p-PI3K, suggesting that silencing LINC01094 suppressed the PI3K/Akt signaling pathway.

In summary, we showed for the first time that LINC01094 exhibited its oncogenic function in PC. LINC01094 promoted PC proliferation and metastasis by acting as a ceRNA for miR-577 to regulate LIN28B expression and the PI3K/Akt pathway, providing new insight into the mechanism of metastatic PC and a novel potential therapeutic target for PC treatment.

MATERIALS AND METHODS

Bioinformatics analysis

Raw and normalized data files for the RNA-seq analysis were retrieved from TCGA dataset (http://gepia.cancer-pku.cn/index.html) in the NCBI Gene Expression Omnibus (GEO) under GEO: GSE15471. The GEO: GSE15471 dataset comprises data from pancreatic ductal adenocarcinoma (PDAC) patients, and the cancer type of the samples used in TCGA dataset was PDAC cancer. The nearby genes of LINC01094 were searched using UCSC (http://genome.ucsc.edu/). The miRNAs that had complementary base-pairing with LINC01094 were predicted by using starBase database (http://starbase.sysu.edu.cn/).

Samples

The PC tissues and pancreatic carcinomas were from 91 patients with PC who were diagnosed at the Second Affiliated Hospital of Nanchang University. The experiments were undertaken with the understanding and written consent of each subject, and the study methodologies conformed to the standards set by the Declaration of Helsinki. This research was approved by the ethics committee of the Second Affiliated Hospital of Nanchang University.

Cell culture

Five human PC cell lines (PANC-1, ASPC-1, BXPC-3, CFPAC-3, and SW1990) and one normal immortalized pancreatic cell line (HPDE6-C7) were purchased from the Shanghai Institute of Cells of the Chinese Academy of Sciences. Cell Bank, using short tandem repeats, was used to identify all of these cells. The cells were routinely cultured in DMEM containing 10% fetal bovine serum (FBS; GIBCO) at 37°C (5% CO_2).

Cell transfection

The LINC01094-overexpressing and shLINC01094-expressing plasmids, the miR-577 mimic (miR-577), and miR-577 negative control (miR-NC) were designed and synthesized by GenePharma (Suzhou, China). Cells transfected with the empty vector were designated or treated as control (named as vector). The LINC01094-specific small interfering RNA (siRNA) and small interfering NC (siNC) were purchased from GenePharma (Shanghai, China). Cell transfection was conducted using Lipofectamine 3000 (Invitrogen, CA, USA). The plasmids and reagents used are described in the Table S1.

Quantitative real-time PCR

Total RNA was extracted from tissue or cultured cells using RNAiso Plus (Takara, Japan), then the RNA was inversely transcribed into cDNA and used for PCR amplification. The results were analyzed by $2^{-\Delta\Delta Ct}$ method. All the primers are in Table S1.

FISH

The FISH Kit was purchased from RiboBio. LINC01094 probes were designed by RiboBio. Transfected PC cells were fixed in 4% paraformaldehyde for 15 min then were permeabilized in PBS containing 0.5% Triton X-100 and prehybridized in hybridization buffer (8 μL 25% dextran sulfate [DS], 20 μL 20x SSC [175.3 g NaCI, 88.2g sodium citrate, 1000 mL H_2O], and 5 μL deionized formamide). Next, cells

and miR-NC/inhibitor and miR-577/inhibitor (**p < 0.01; scale bar, 100 μm). (I and J) PC cell invasion and migration were measured through wound-healing (I) and transwell (J) assays in PC cells transfected with miR-NC/mimic and miR-577/mimic and miR-NC/inhibitor and miR-577/inhibitor (**p < 0.01; scale bar, 100 μm). (K) The elevated expression of LIN28B in tissue levels was detected by IHC test and normalized to the PC tissue group (**p < 0.01; scale bar, 100 μm). (L) Scatterplots show a positive correlation between LINC01094 and LIN28B at the mRNA levels in 91 PC tissues (r = 0.4918, **p < 0.01); those among multiple groups were analyzed by the one-way ANOVA or repeated-measures ANOVA. Correlation analysis between two groups was conducted using Pearson's correlation analysis. The experiment was repeated three times (mean ± SEM).

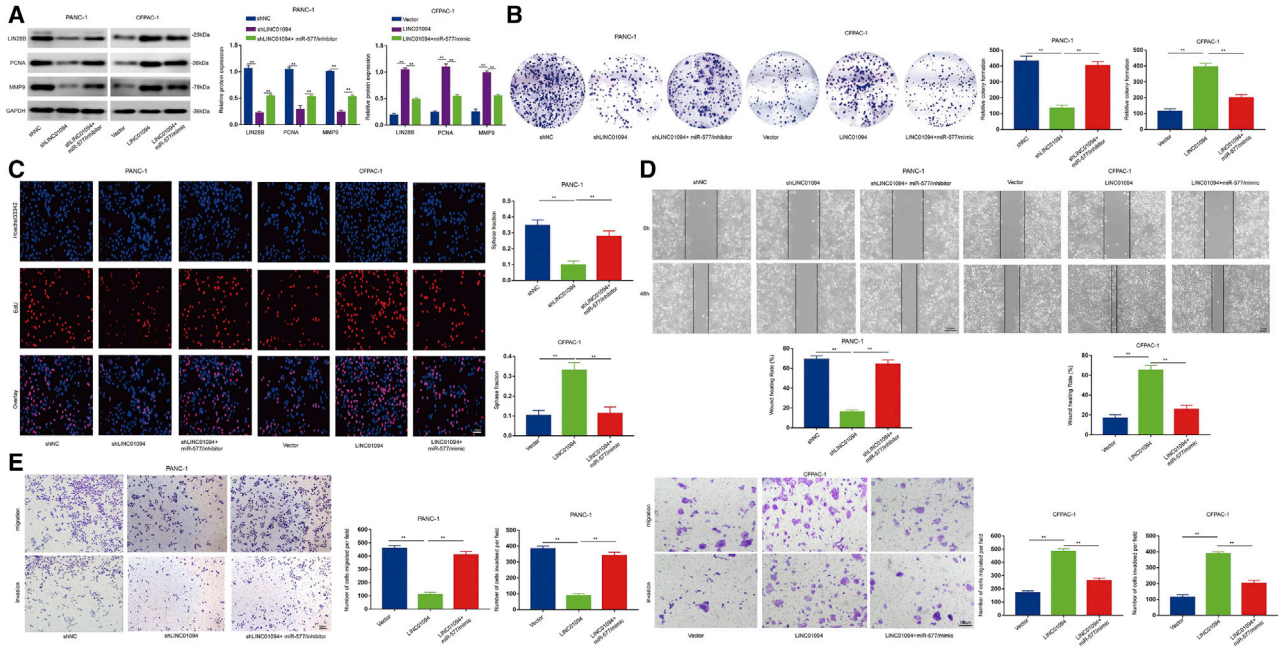

Figure 6. LINC01094 acts as a sponge of miR-577 to upregulating LIN28B expression

(A) Western blotting analysis of proliferation-associated antigens in PANC-1 and CFPAC-1 cells stably transfected with shNC, shLINC01094, shLINC01094+miR-577/inhibitor and vector, LINC01094, and LINC01094+miR-577/mimic. (B and C) Clone formation (B) and EdU (C) assays were performed to determine the mobility capacity of PANC-1 and CFPAC-1 cells stably transfected with shNC, shLINC01094, shLINC01094+miR-577/inhibitor and vector, LINC01094, and LINC01094+miR-577/mimic (**$p < 0.01$; scale bar, 100 μm). (D and E) Wound-healing (D) and transwell (E) assays were performed to determine the mobility capacity of PANC-1 and CFPAC-1 cells stably transfected with shNC, shLINC01094, shLINC01094+miR-577/inhibitor and vector, LINC01094, and LINC01094+miR-577/mimic (**$p < 0.01$; scale bar, 100 μm); those among multiple groups were analyzed by the one-way ANOVA or repeated-measures ANOVA. The experiment was repeated three times (mean ± SEM).

were further incubated with 50 nM of the probe in hybridization buffer at 4°C overnight. The next day, cells were washed with PBS and counterstained with 4′, 6-diamidino-2-phenylindole (DAPI). All images were analyzed on a confocal laser scanning microscope (Leica Microsystems, Mannheim, Germany). The FISH probe sequences are shown as follows: LINC01094: 5′-TAGATTTAACTGC CTAACTAACGATGAAGC-3′.

Western blotting

As mentioned earlier, western blotting analysis was performed.[45] The antibodies in this study are as follows: rabbit antibody LIN28B (1:5,00, ab46020, Abcam); rabbit antibody PCNA (1:1,000, ab92552, Abcam); rabbit antibody MMP9 (1:1,000, ab137867, Abcam); rabbit antibody Akt (1:1,000, ab8805, Abcam); rabbit antibody p-Akt (1:1,000, ab38449, Abcam); rabbit antibody PI3K (1:1,000, ab32089, Abcam); rabbit antibody p-PI3K (1:1,000, ab278545, Abcam); and mouse antibody GAPDH (1:1,000, ab9484, Abcam).

Immunohistochemistry (IHC) analysis

IHC analysis of LIN28B, PCNA, and MMP9 procedures were performed as described previously.[46] Antibodies used were as follows: rabbit antibody PCNA (1:2,00, ab92552, Abcam), rabbit antibody LIN28B (1:2,00, ab262858, Abcam), and rabbit antibody MMP9 (1:2,00, ab137867, Abcam).

Colony formation assay

Transfected PC cells were seeded in 6 well plates with a total of 500 cells per well. After 2 weeks of incubation, they were fixed with 4% paraformaldehyde then incubated with crystal violet for 15 min and counted under the microscope.

EdU assay

The cells were incubated with EdU (Ribobio) for 5 h. After three rinses with PBS, the cells were treated with 300 mL of 1 × Apollo reaction cocktail for 30 min. The DNA content of the cells in each well was then stained with 100 mL of Hoechst 33342 (5 mg/ml) for 30 min. Subsequently, the cells were visualized under a fluorescence microscope.

Wound-healing assay

The wound-healing rate was determined by a scratch test to evaluate the ability of cell migration, which was briefly described as follows: cells were inoculated in a 6-well plate to form a monolayer and scratched with a sterile pipette (200 μL). Loose cell fragments were washed with PBS, and the remaining cells were cultured for 0 h and 48 h. Then, the wound images were taken by microscope, and the migration distance of the monolayer growth edge at 24 h after injury was observed, and the wound-healing rate was calculated.

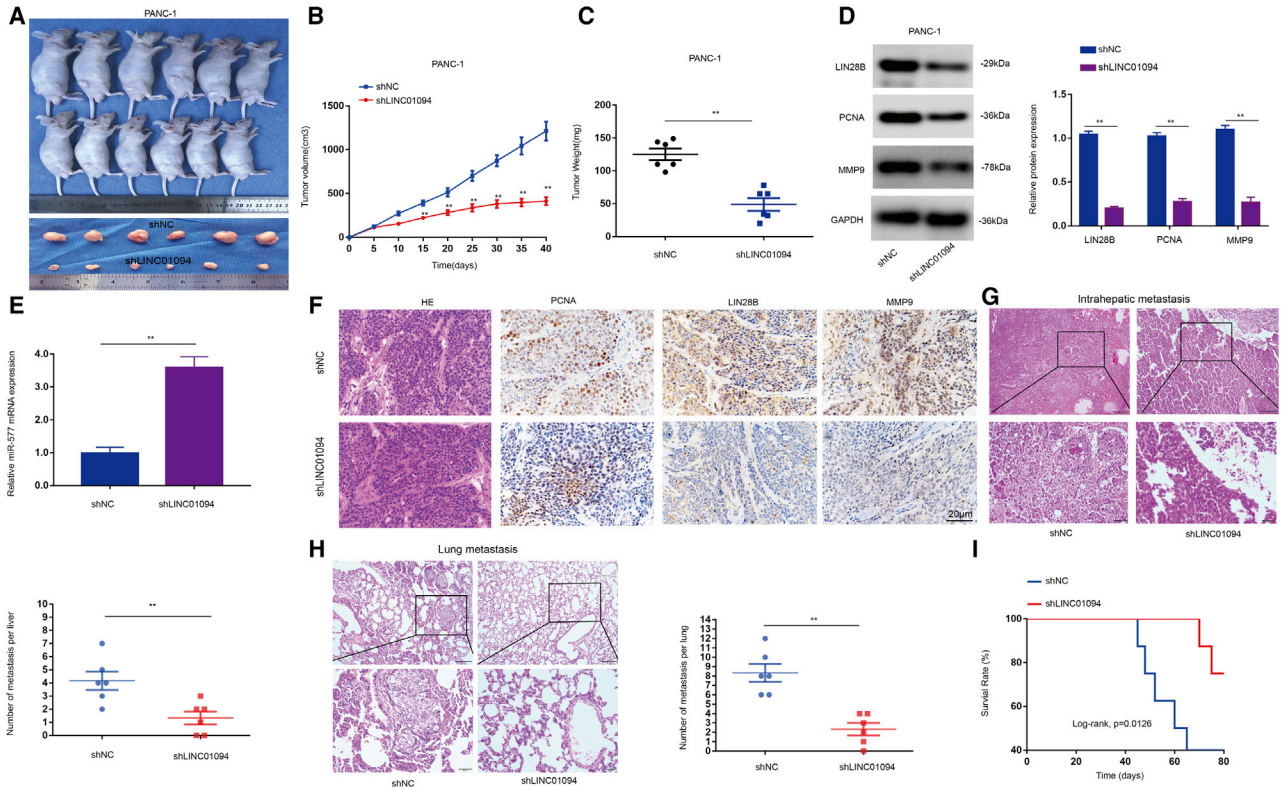

Figure 7. Silencing of LINC01094 suppresses the proliferation and metastasis of PC cells *in vivo*

(A) Forty days after injection, the nude mice were killed and the tumors in each group were shown. (B and C) The tumor growth curve was observed after subcutaneous injection of PNAC-1 cells expressing shNC or shLINC01094, and the tumor volume (B) and weight (C) were measured in mouse xenografts (mean ± SEM; n = 6; **p < 0.01; scale bar, 100 μm). Data are representative of at least three independent experiments. (D) Relative expression levels of MMP9, PNCA, and LIN28B are observed in subcutaneous tumor tissues by western blot assays. (E) PANC-1 tumor samples from shNC- and shLINC01094-treated mice were analyzed by quantitative real-time PCR (**p < 0.01). (F) PANC-1 tumor samples from shNC- and shLINC01094-treated mice were immunohistochemically stained for LIN28B, MMP9, and PCNA (scale bars, 20 μm). (G and H) Sections with metastatic nodules in the liver (G) and lung (H) were stained with H&E, and then the number of metastatic nodules was analyzed (**p < 0.01; scale bar, 100 μm). (I) Kaplan-Meier survival curves for mice of the PANC-1-shLINC01094 group and control group (p = 0.00126); data were expressed as mean ± SD and analyzed using unpaired t test. The experiment was repeated three times.

Transwell assay

Three groups of cells were inoculated on the transwell chamber with 1×10^4 cells per group. After 24 h of culture, formaldehyde was fixed through the cells under the ependyma, and the staining solution was 0.2% crystal violet solution and enumerated it under the microscope.

Subcellular fractionation assay

PANC-1 and ASPC-1 cell lines were collected in a cell fractionation buffer using PARIS Kit (Invitrogen, USA). PBS washed the cell fragments. A cell fractionation buffer was used to place the cell lysates and centrifuged. The isolated RNA was used for PCR amplification. The cytoplasmic and nuclear fractionation indicators used were GAPDH and U6, respectively.

Luciferase reporter gene assay

The WT-LINC01094 and the WT-LIN28B with a predicted binding site of miR-577 and the promoter region of Mut-LINC01094 and Mut-LIN28B were synthesized and cloned into luciferase reporter vector pGL3 (Promega, Madison, WI, USA). The PC cells were co-transfected with corresponding reporter plasmids and miR-577 mimic or NC mimic by Lipofectamine 3000 and were detected by the double luciferase report method.

RIP

Resulting transfected cells were lysed with radioimmunoprecipitation assay (RIPA) buffer, centrifuged at 14,000 rpm for 15 min, and then incubated overnight at 4°C, with shaking prior to addition of 10 μL beads and 2 μL Ago2 antibody. The mixture was rinsed twice using a lysis buffer, and Trizol reagent (Invitrogen) was used to extract RNA from the lysed cells.

In vivo tumor growth and metastasis assay

The 6- to 8-week-old nude male mice were purchased from the Institute of Model Zoology, Nanjing University. All experiments were performed in accordance with the NIH guidelines for the humane care

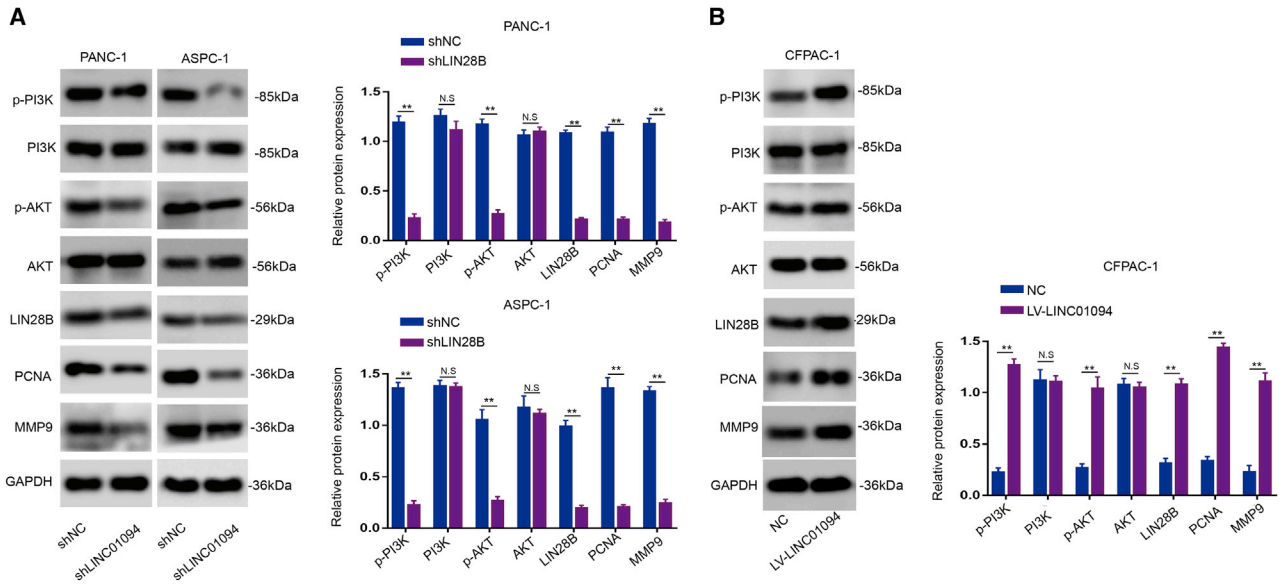

Figure 8. Silencing LINC01094 suppresses the expression of the PI3K/Akt signaling pathway in PC cells

(A) The effects of LINC01094 gene silencing on the expression of PI3K, p-PI3K, p-Akt, and Akt in PANC-1 and ASPC-1 cells were detected by western blot analysis. **$p < 0.01$ compared with the shNC group. (B) The effects of LINC01094 gene upregulated on the expression of PI3K, p-PI3K, p-Akt, and Akt in CFPAC-1 cells was detected by western blot analysis. **$p < 0.01$ compared with the vector group; data were expressed as mean ± SD and analyzed using unpaired t test. The experiment was repeated three times.

and use of laboratory animals and were approved by the Institutional Animal Care and Use Committee at Nanchang University. The cell concentration was adjusted to 1×10^6 cells/mL. After the skin of the back of nude mice was disinfected with 75% alcohol, 0.2 mL cell suspension was injected into the back and the intrasplenical region of nude mice to establish the model of ectopic tumor formation of PC cells in nude mice. The general health status and tumor growth of nude mice were observed regularly, and the volume and weight of the transplanted tumor were recorded.

Statistical analysis

SPSS 22.0 (IBM, SPSS, Chicago, IL, USA) software and GraphPad Prism 7.0 (GraphPad Software, San Diego, CA, USA) were used to statistically process the data, and all results were displayed as means ± standard deviation (SD). Student's t test was used for comparison between two groups while more than two groups were analyzed by one-way analysis of variance (ANOVA) and post hoc test to correct for multiple comparisons. Spearman correlation analysis was used for correlation, and $p < 0.05$ was set as the threshold for statistical significance.

SUPPLEMENTAL INFORMATION

Supplemental information can be found online at https://doi.org/10.1016/j.omtn.2021.08.024.

ACKNOWLEDGMENTS

This work was supported by the National Natural Science Foundation of China (no. 81560389); the Project of the Jiangxi Provincial Department of Science and Technology (nos. 20181BBG70015 and 20202BABL206091); the Project of the Jiangxi Provincial Education Department of Science and Technology Research (no. 180075); the Project of the Jiangxi Provincial Department of Health and Family Planning Commission Science and Technology Plan Research (no. 20171068); the Project of the Jiangxi Provincial Department of Science and Technology Plan of Health and Health Commission (no. 20204359); and the Project of Jiangxi Provincial Innovation Fund for Graduate Students (no. YC2019-B014).

AUTHOR CONTRIBUTIONS

C.L. and Z.Z. designed the experiments and wrote the paper. C.L., K.L., and X.Z. conducted the experiments. K.L., X.Z., and J.Z. analyzed the data. C.L., C.H., and J.Z., revised the figures and tables. K.L., X.Z., and J.Z. collected the tissue samples and clinical data of PC patients.

DECLARATION OF INTERESTS

The authors declare no competing interests.

REFERENCES

1. Jooste, V., Dejardin, O., Bouvier, V., Arveux, P., Maynadie, M., Launoy, G., and Bouvier, A.M. (2016). Pancreatic cancer: Wait times from presentation to treatment and survival in a population-based study. Int. J. Cancer *139*, 1073–1080.

2. Puleo, F., Maréchal, R., Demetter, P., Bali, M.A., Calomme, A., Closset, J., Bachet, J.B., Deviere, J., and Van Laethem, J.L. (2015). New challenges in perioperative management of pancreatic cancer. World J. Gastroenterol. *21*, 2281–2293.

3. Garrido-Laguna, I., and Hidalgo, M. (2015). Pancreatic cancer: from state-of-the-art treatments to promising novel therapies. Nat. Rev. Clin. Oncol. *12*, 319–334.

4. Siegel, R.L., Miller, K.D., and Jemal, A. (2018). Cancer statistics, 2018. CA Cancer J. Clin. *68*, 7–30.

5. Campbell, P.J., Yachida, S., Mudie, L.J., Stephens, P.J., Pleasance, E.D., Stebbings, L.A., Morsberger, L.A., Latimer, C., McLaren, S., Lin, M.L., et al. (2010). The patterns

and dynamics of genomic instability in metastatic pancreatic cancer. Nature *467*, 1109–1113.

6. Batista, P.J., and Chang, H.Y. (2013). Long noncoding RNAs: cellular address codes in development and disease. Cell *152*, 1298–1307.
7. Guttman, M., Amit, I., Garber, M., French, C., Lin, M.F., Feldser, D., Huarte, M., Zuk, O., Carey, B.W., Cassady, J.P., et al. (2009). Chromatin signature reveals over a thousand highly conserved large non-coding RNAs in mammals. Nature *458*, 223–227.
8. Nagano, T., and Fraser, P. (2011). No-nonsense functions for long noncoding RNAs. Cell *145*, 178–181.
9. Ponting, C.P., Oliver, P.L., and Reik, W. (2009). Evolution and functions of long noncoding RNAs. Cell *136*, 629–641.
10. Ulitsky, I., and Bartel, D.P. (2013). lincRNAs: genomics, evolution, and mechanisms. Cell *154*, 26–46.
11. Kallen, A.N., Zhou, X.B., Xu, J., Qiao, C., Ma, J., Yan, L., Lu, L., Liu, C., Yi, J.S., Zhang, H., et al. (2013). The imprinted H19 lncRNA antagonizes let-7 microRNAs. Mol. Cell *52*, 101–112.
12. Schmitt, A.M., and Chang, H.Y. (2016). Long Noncoding RNAs in Cancer Pathways. Cancer Cell *29*, 452–463.
13. Chen, L.L. (2016). Linking Long Noncoding RNA Localization and Function. Trends Biochem. Sci. *41*, 761–772.
14. Zhang, D., Zhang, G., Hu, X., Wu, L., Feng, Y., He, S., Zhang, Y., Hu, Z., Yang, L., Tian, T., et al. (2017). Oncogenic RAS Regulates Long Noncoding RNA *Orilnc1* in Human Cancer. Cancer Res. *77*, 3745–3757.
15. Lu, Y., Hu, Z., Mangala, L.S., Stine, Z.E., Hu, X., Jiang, D., Xiang, Y., Zhang, Y., Pradeep, S., Rodriguez-Aguayo, C., et al. (2018). MYC Targeted Long Noncoding RNA DANCR Promotes Cancer in Part by Reducing p21 Levels. Cancer Res. *78*, 64–74.
16. Peng, W., Gao, W., and Feng, J. (2014). Long noncoding RNA HULC is a novel biomarker of poor prognosis in patients with pancreatic cancer. Med. Oncol. *31*, 346.
17. Sun, J., Zhang, P., Yin, T., Zhang, F., and Wang, W. (2020). Upregulation of LncRNA PVT1 Facilitates Pancreatic Ductal Adenocarcinoma Cell Progression and Glycolysis by Regulating MiR-519d-3p and HIF-1A. J. Cancer *11*, 2572–2579.
18. Bi, S., Wang, Y., Feng, H., and Li, Q. (2020). Long noncoding RNA LINC00657 enhances the malignancy of pancreatic ductal adenocarcinoma by acting as a competing endogenous RNA on microRNA-433 to increase PAK4 expression. Cell Cycle *19*, 801–816.
19. Jiang, Y., Zhang, H., Li, W., Yan, Y., Yao, X., and Gu, W. (2020). FOXM1-Activated LINC01094 Promotes Clear Cell Renal Cell Carcinoma Development via MicroRNA 224-5p/CHSY1. Mol. Cell. Biol. *40*, e00357-19.
20. Zhang, W., Shen, C., Li, C., Yang, G., Liu, H., Chen, X., Zhu, D., Zou, H., Zhen, Y., Zhang, D., and Zhao, S. (2016). miR-577 inhibits glioblastoma tumor growth via the Wnt signaling pathway. Mol. Carcinog. *55*, 575–585.
21. Wang, L.Y., Li, B., Jiang, H.H., Zhuang, L.W., and Liu, Y. (2015). Inhibition effect of miR-577 on hepatocellular carcinoma cell growth via targeting β-catenin. Asian Pac. J. Trop. Med. *8*, 923–929.
22. Kugel, S., Sebastián, C., Fitamant, J., Ross, K.N., Saha, S.K., Jain, E., Gladden, A., Arora, K.S., Kato, Y., Rivera, M.N., et al. (2016). SIRT6 Suppresses Pancreatic Cancer through Control of Lin28b. Cell *165*, 1401–1415.
23. Moss, E.G., Lee, R.C., and Ambros, V. (1997). The cold shock domain protein LIN-28 controls developmental timing in C. elegans and is regulated by the lin-4 RNA. Cell *88*, 637–646.
24. Liu, Y., Wang, D., Zhou, M., Chen, H., Wang, H., Min, J., Chen, J., Wu, S., Ni, X., Zhang, Y., et al. (2021). The KRAS/Lin28B axis maintains stemness of pancreatic cancer cells via the let-7i/TET3 pathway. Mol. Oncol. *15*, 262–278.
25. Ustianenko, D., Chiu, H.S., Treiber, T., Weyn-Vanhentenryck, S.M., Treiber, N., Meister, G., Sumazin, P., and Zhang, C. (2018). LIN28 Selectively Modulates a Subclass of Let-7 MicroRNAs. Mol. Cell *71*, 271–283.e5.
26. Joshi, S., Wei, J., and Bishopric, N.H. (2016). A cardiac myocyte-restricted Lin28/let-7 regulatory axis promotes hypoxia-mediated apoptosis by inducing the AKT signaling suppressor PIK3IP1. Biochim. Biophys. Acta *1862*, 240–251.
27. Chen, C., Bai, L., Cao, F., Wang, S., He, H., Song, M., Chen, H., Liu, Y., Guo, J., Si, Q., et al. (2019). Targeting LIN28B reprograms tumor glucose metabolism and acidic microenvironment to suppress cancer stemness and metastasis. Oncogene *38*, 4527–4539.
28. Zhang, R., Sun, S., Ji, F., Liu, C., Lin, H., Xie, L., Yang, H., Tang, W., Zhou, Y., Xu, J., et al. (2017). CNTN-1 Enhances Chemoresistance in Human Lung Adenocarcinoma Through Induction of Epithelial-Mesenchymal Transition by Targeting the PI3K/Akt Pathway. Cell Physiol. Biochem. *43*, 465–480.
29. Zhang, Y., Chen, P., Yin, W., Ji, Y., Shen, Q., and Ni, Q. (2018). Nectin-4 promotes gastric cancer progression via the PI3K/AKT signaling pathway. Hum. Pathol. *72*, 107–116.
30. Duru, N., Wolfson, B., and Zhou, Q. (2016). Mechanisms of the alternative activation of macrophages and non-coding RNAs in the development of radiation-induced lung fibrosis. World J. Biol. Chem. *7*, 231–239.
31. Hammond, S.M. (2015). An overview of microRNAs. Adv. Drug Deliv. Rev. *87*, 3–14.
32. Carlevaro-Fita, J., Lanzós, A., Feuerbach, L., Hong, C., Mas-Ponte, D., Pedersen, J.S., and Johnson, R.; PCAWG Drivers and Functional Interpretation Group; PCAWG Consortium (2020). Cancer LncRNA Census reveals evidence for deep functional conservation of long noncoding RNAs in tumorigenesis. Commun. Biol. *3*, 56.
33. Gutschner, T., and Diederichs, S. (2012). The hallmarks of cancer: a long non-coding RNA point of view. RNA Biol. *9*, 703–719.
34. Prensner, J.R., and Chinnaiyan, A.M. (2011). The emergence of lncRNAs in cancer biology. Cancer Discov. *1*, 391–407.
35. Ren, X., Chen, C., Luo, Y., Liu, M., Li, Y., Zheng, S., Ye, H., Fu, Z., Li, M., Li, Z., and Chen, R. (2020). lncRNA-PLACT1 sustains activation of NF-κB pathway through a positive feedback loop with IκBα/E2F1 axis in pancreatic cancer. Mol. Cancer *19*, 35.
36. Chen, B., Zhang, Q., Wang, X., Wang, Y., Cui, J., Zhuang, H., and Tang, J. (2020). The lncRNA ENSG00000254041.1 promotes cell invasiveness and associates with poor prognosis of pancreatic ductal adenocarcinoma. Aging (Albany NY) *12*, 3647–3661.
37. Bayoumi, A.S., Sayed, A., Broskova, Z., Teoh, J.P., Wilson, J., Su, H., Tang, Y.L., and Kim, I.M. (2016). Crosstalk between Long Noncoding RNAs and MicroRNAs in Health and Disease. Int. J. Mol. Sci. *17*, 356.
38. Dhanoa, J.K., Sethi, R.S., Verma, R., Arora, J.S., and Mukhopadhyay, C.S. (2018). Long non-coding RNA: its evolutionary relics and biological implications in mammals: a review. J. Anim. Sci. Technol. *60*, 25.
39. Guo, D., Li, Y., Chen, Y., Zhang, D., Wang, X., Lu, G., Ren, M., Lu, X., and He, S. (2019). DANCR promotes HCC progression and regulates EMT by sponging miR-27a-3p via ROCK1/LIMK1/COFILIN1 pathway. Cell Prolif. *52*, e12628.
40. Sun, Y., Jia, X., Wang, M., and Deng, Y. (2019). Long noncoding RNA MIR31HG abrogates the availability of tumor suppressor microRNA-361 for the growth of osteosarcoma. Cancer Manag. Res. *11*, 8055–8064.
41. Niu, L., Zhou, Y., Zhang, W., and Ren, Y. (2019). Long noncoding RNA LINC00473 functions as a competing endogenous RNA to regulate MAPK1 expression by sponging miR-198 in breast cancer. Pathol. Res. Pract. *215*, 152470.
42. Wang, C., Gu, Y., Zhang, E., Zhang, K., Qin, N., Dai, J., Zhu, M., Liu, J., Xie, K., Jiang, Y., et al. (2019). A cancer-testis non-coding RNA LIN28B-AS1 activates driver gene LIN28B by interacting with IGF2BP1 in lung adenocarcinoma. Oncogene *38*, 1611–1624.
43. Wang, T., Wang, G., Hao, D., Liu, X., Wang, D., Ning, N., and Li, X. (2015). Aberrant regulation of the LIN28A/LIN28B and let-7 loop in human malignant tumors and its effects on the hallmarks of cancer. Mol. Cancer *14*, 125.
44. Ji, W., Diao, Y.L., Qiu, Y.R., Ge, J., Cao, X.C., and Yu, Y. (2020). LINC00665 promotes breast cancer progression through regulation of the miR-379-5p/LIN28B axis. Cell Death Dis. *11*, 16.
45. Li, Q., Chen, L., Luo, C., ChenYan, Ge, J., Zhu, Z., Wang, K., Yu, X., Lei, J., Liu, T., et al. (2020). TAB3 upregulates PIM1 expression by directly activating the TAK1-STAT3 complex to promote colorectal cancer growth. Exp. Cell Res. *391*, 111975.
46. Luo, C., Yuan, R., Chen, L., Zhou, W., Shen, W., Qiu, Y., Shao, J., Yan, J., and Shao, J. (2017). TAB3 upregulates Survivin expression to promote colorectal cancer invasion and metastasis by binding to the TAK1-TRAF6 complex. Oncotarget *8*, 106565–106576.